physical sciences forum

Proceeding Paper

Structure Functions and Tau Neutrino Cross Section at DUNE Far Detector †

Barbara Yaeggy

Department of Physics, University of Cincinnati, Cincinnati, OH 45221, USA; yaeggyba@ucmail.uc.edu or byaeggy@gmail.com

† Presented at the 23rd International Workshop on Neutrinos from Accelerators, Salt Lake City, UT, USA, 30–31 July 2022.

Abstract: DUNE's Argon time-projecting chambers (TPC) detectors will allow us to conduct precise studies about phenomena that have, until now, seemed too challenging to measure, like tau neutrino (ν_τ) interactions. Cross section measurements are needed to understand how accurate our neutrino-nucleus interaction models are and how accurately we can use them to reconstruct neutrino energy. Quasi-elastic scattering (QE), Δ resonance production (RES), and deep inelastic scattering (DIS) processes are known to provide dominant contributions in the medium and high neutrino energy to the total cross-section of ν_τ(N) and $\bar{\nu}_\tau$(N). These cross-sections have large systematic uncertainties compared to the ones measured for ν_μ and ν_e and their antiparticles. Studies point out that the reason for these differences is due to the model dependence of the ν_τ(N) cross-sections in treating the nuclear medium effects described by the nucleon structure functions, $F_{1N,\ldots,3N}(x,Q^2)$ for ν_μ and ν_e. These proceedings show the semi-theoretical and experimental approach to the estimation of the ν_τ(N) and $\bar{\nu}_\tau$(N) cross-sections in DUNE for the DIS region. We will check the contributions of the additional nucleon structure functions $F_{4N}(x,Q^2)$ and $F_{5N}(x,Q^2)$ and their dependence on Q^2 and Bjorken-x scale.

Keywords: neutrino; nutau; tau; structure functions; interactions; cross section; TPC detectors; DUNE; machine learning; semantic segmentation; panoptic segmentation

Citation: Yaeggy, B. Structure Functions and Tau Neutrino Cross Section at DUNE Far Detector. *Phys. Sci. Forum* **2023**, *8*, 64. https://doi.org/10.3390/psf2023008064

Academic Editor: Yue Zhao

Published: 17 October 2023

1. Introduction

The current generation of neutrino experiments have provided a nearly complete description of the three flavor paradigm, but almost all knowledge of the tau neutrino sector is taken from lepton universality for cross sections and the unitarity of the Pontecorvo–Maki–Nakagawa–Sakata (PMNS) matrix for oscillations (an indirect way); it is critical that these assumptions are tested in a direct way and DUNE will be able to provide the data to analyze and disentangle the last piece of the puzzle, the physics of the tau neutrino.

The DUNE Far Detector (FD), currently under construction, will consist of four 10 kt fiducial mass LArTPC modules located at a baseline of 1285 km from the LBNF neutrino source at the 4850 km level of the Sanford Underground Research Facility in Lead, South Dakota. The long baseline, large detector mass, and intense beam will allow DUNE to measure all three flavor oscillation parameters in a single experiment. While DUNE is optimized to measure ν_e appearance in a ν_μ beam, the broadband beam and long baseline lead to significant ν_τ appearance above the kinematic threshold to produce a τ-lepton, Ref. [1]. DUNE is the only upcoming neutrino experiment expected to be able to collect a larger sample of oscillated ν_τ events from a beam than all previous experiments.

A truthlevel study of ν_τ-CC interactions in Ref. [2], where the τ-lepton decayed hadronically, suggests that relatively simple kinematic requirements of events containing at least one $\pi^\pm$ could confirm ν_τ-CC appearance with a significance of 3.1σ in one year of running in the CP-optimized beam mode or 7.9σ in one year of running in the tau-optimized beam mode, assuming 1.2 MW beam power and 40 kt fiducial mass, see Figure 1. This selection corresponds to $\sim$60% signal efficiency and $\sim$80% NC background rejection efficiency. The expected counts per year for the CP-optimized neutrino mode are $\approx$30 $\bar{\nu_\tau}$ and $\approx$130 ν_τ and for the tau optimized neutrino mode they are expected to be $\approx$800 ν_τ.

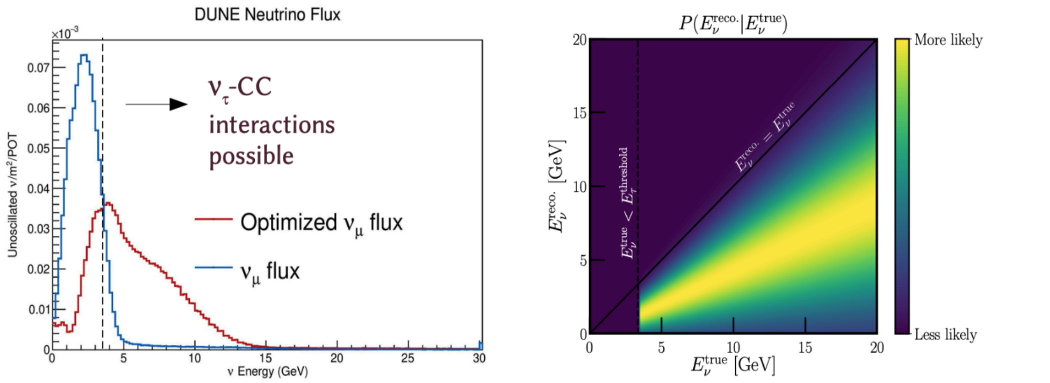

Figure 1. (**Left**): in blue, CP-optimized beam, here the design requires a 3 horns configuration; in red, tau-optimized beam, the design requires a 2 horns configuration. This is a future upgrade, and it is under investigation. (**Right**): Migration matrix for hadronically decaying τ leptons produced via ν_τ-CC interactions. The assumed bias is 45% and the resolution is 25%. No migration exists below $E_\nu^{true} \approx 3.4$ GeV, as the scattering process is kinematically forbidden, Ref. [3].

Quasi-elastic scattering (QE), Δ resonance production (RES), and deep inelastic scattering (DIS) processes are known to provide dominant contributions at medium and high neutrino energy to the total cross section of ν_τ(N) and $\bar{\nu}_\tau$(N) cross sections. These cross sections have large systematic uncertainties compared to the ones for ν_μ and ν_e. Studies point out that the reason for these differences is the model dependence of the ν_τ(N) cross sections in treating the nuclear medium effects described by the nucleon structure functions, $F_{1N,...,3N}(x, Q^2)$ for ν_μ and ν_e. These nucleon structure functions are used to calculate DIS cross section by including kinematic corrections, but due to the addition of the τ-lepton mass another two additional nucleon structure functions become non-negligible, $F_{4N}(x, Q^2)$ and $F_{5N}(x, Q^2)$.

2. DIS ν_τ-CC cross Section

Neutrino interactions are a major contributor to systematic uncertainties in oscillation measurements (T2K, NOvA). The measurement of the E_ν and ν-nucleus interactions relies on reconstruction techniques based either on kinematics (T2K, HK) or calorimetric methods (DUNE, NOvA, SBN); both techniques require reliable predictions from the *interaction models*. Now, it turns out that, when it comes to oscillations, the extraction of the oscillation parameter is biased by the *interaction models* as well because it is E_ν dependent, see Equation (1). On the other hand, the number of events detected is proportional to such probability, flux, and cross section, which at the same time are E_ν-dependent, see Equation (2). Notice that nuclear and hadronic effects are E_ν-dependent as well; therefore, obtaining reliable predictions from the interaction models is necessary, and how do we attain access to study those—through cross section measurements.

$$P_{\nu_\alpha \to \nu_\beta} = sin^2 2\theta_i sin^2 \left(\frac{\Delta m_i^2 L}{4E_\nu} \right) \tag{1}$$

$$N_{FD}^{\alpha \to \beta}(E_\nu, rec) \propto \sum_i \phi_\alpha(E_\nu) \times \sigma_\beta^i(E_\nu) \times P_{\nu_\alpha \to \nu_\beta} \times \epsilon_\beta(E_\nu, E_{\nu,rec}). \tag{2}$$

2.1. Tau Neutrino Interactions

Due to the large mass of the $\tau^{\pm}$ relative to the $e^{\pm}$ and $\mu^{\pm}$, the threshold for this process to occur is 3.5 GeV (see Figure 1).

Surveys of various decay modes of the tau lepton are dominant in the study of tau neutrino physics, see those branching ratios in Table 1. The leptonic decay channels of the tau are more challenging than their hadronic peers; this happens because the background from CC interactions (ν_e and ν_μ) is larger than the neutral current (NC) background, and also because the tau decays to charged leptons at approximately half the rate it decays to hadrons.

Table 1. Dominant decay modes of τ^-. Kaonic decays and others go into the "other" category, Ref [2].

Decay Mode	Branching Ratio (%)
Leptonic	35.2
$e^-\bar{\nu}_e\,\nu_\tau$	17.3
$\mu^-\bar{\nu}_\mu\,\nu_\tau$	17.4
Hadronic	64.8
$\pi^-\pi^0\nu_\tau$	25.5
$\pi^-\nu_\tau$	10.8
$\pi^-\pi^0\pi^0\nu_\tau$	9.3
$\pi^-\pi^-\pi^+\nu_\tau$	9.0
$\pi^-\pi^-\pi^+\pi^0\,\nu_\tau$	4.5
other	5.7

2.2. Structure Functions

A structure function (SF) characterizes the internal structure of the nucleon; the contributions of the SF to the cross section are functions of the charged lepton mass. In 1975, Albright and Jarlskog [4] pointed out that there are two additional structure functions—F_4 and F_5—that contribute to the ν_τ-CC cross section, a key input to theoretical and experimental analyses of tau neutrino. F_4 and F_5 are ignored in muon neutrino interactions because of a suppression factor depending on $m_l^2/(M_N E_\nu)$, where M_N and m_l^2 are the nucleon and lepton mass, respectively. At leading order, in the limit of massless quarks and target, F_4 and F_5 are:

$$F_4 = 0 \quad and \quad 2xF_5 = F_2, \tag{3}$$

where x is the Bjorken-x variable. These generalizations of the Callan–Gross relation $F_2 = 2xF_1$ are called the Albright–Jarlskog (AJ) relations.

Neglecting neither the target nucleon mass M_N nor the final state lepton mass m_τ, the ν_τ (anti-)neutrino CC differential cross section is represented by a standard set of five structure functions [5]:

$$\begin{aligned}\frac{d^2\sigma_A}{dxdy} = \quad & \frac{G_F^2 M_N E_\nu}{\pi\left(1+\frac{Q^2}{M_W^2}\right)^2}\Bigg\{\left[y^2x+\frac{m_l^2 y}{2E_\nu M_N}\right]F_{1A}(x,Q^2) \\ & +\left[\left(1-\frac{m_l^2}{4E_\nu^2}\right)-\left(1+\frac{M_N x}{2E_\nu}\right)y\right]F_{2A}(x,Q^2) \\ & \pm\left[xy\left(1-\frac{y}{2}\right)\right]F_{3A}(x,Q^2)+\frac{m_l^2(m_l^2+Q^2)}{4E_\nu^2 M_N^2 x}F_{4A}(x,Q^2) \\ & -\frac{m_l^2}{E_\nu M_N}F_{5A}(x,Q^2)\Bigg\},\end{aligned} \tag{4}$$

where x, y, Q^2 are the standard DIS kinematic variables related through $Q^2 = 2M_N E_\nu xy$.

Notice that, in Equation (4), in the limit $m_l^2 \to 0$, only F_1, F_2 and F_3 contribute. Once again, given the higher mass value of the *tau* lepton, F_4 and F_5 pointed out by (AJ) relations occur only in heavy lepton (τ) scattering and are negligible for ν_μ and ν_e, but become important for ν_τ cross section. Notice that $F_4 = 0$ also holds when the nucleon target is replaced by a lepton target.

Figure 2 (both panels) shows that, in evaluations of the total CC cross section, the naive AJ relations are good approximations to the NLO results. This is true at low energies, where the ν_τ cross section does not probe small-x, and at high energies where F_4, F_5 are suppressed, anyway.

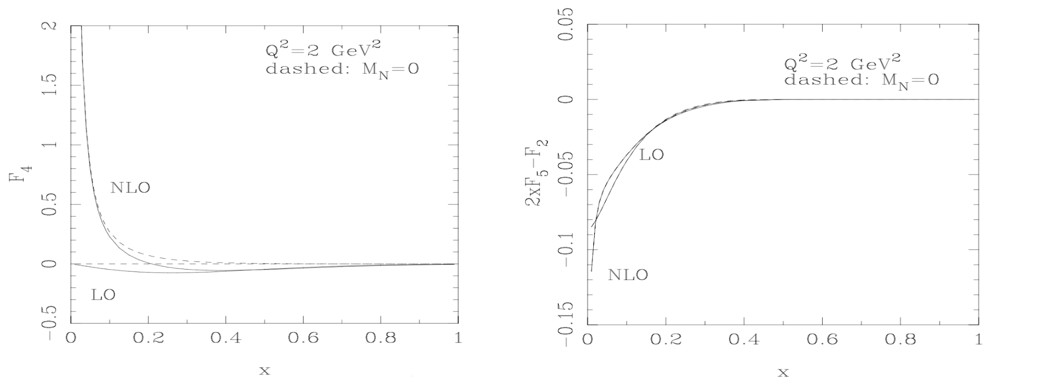

Figure 2. (**Left**): F_4, the LO curve with $M_N = 0$ shows that $F_4 = 0$, at NLO, $F_4 \approx 1\%$ of F_5; therefore, the AJ relations are good approximations to the NLO result. (**Right**): F_5, at LO, AJ relation is violated, $2xF_5 - F_2 \neq 0$; this is due to the charm quark mass corrections; NLO corrections have an effect primarily at small-x [6].

3. Preliminary Results and Outlook

Following Equation (4), we use the tau-optimized beam flux simulation with the DUNE far detector geometry and Genie 3.0.6 [7]. The cross section for the tau (anti) neutrino for the standard model (SM) prediction and the $F_4 = 0, F_5 = 0$ hypothesis is shown in Figure 3, the SM prediction being smaller than the $F_4 = 0, F_5 = 0$ hypothesis. From Figure 2, the effect from F_4 can be discarded, but what about F_5?

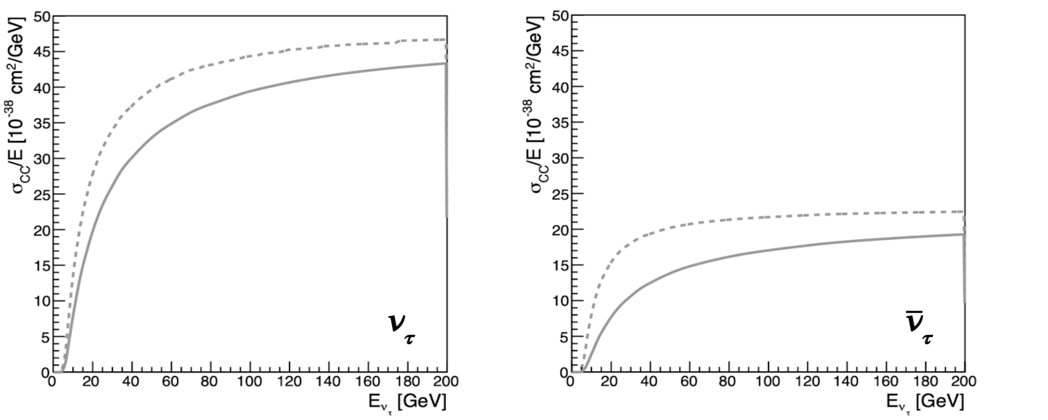

Figure 3. (**Left**), ν_τ and (**right**), ν_τ-CC cross sections. Notice the difference between the cross sections in the $F_4 = 0, F_5 = 0$ hypothesis (dashed line) and the standard model prediction (solid line).

$F_5(x, Q^2)$ Nature

The effect of F_5 in the $[x, Q^2]$ phase space as a function of the number of events can be appreciated in Figure 4. On the left side, we have the SM prediction, and on the right, the case when $F_4 = F_5 = 0$, notice the changes between $x = 0.2 - 0.5$, we can access a higher number of statistics and therefore, to get the chance to study nuclear interactions deeper. Based on what Figure 4 shows, we go to check over the $[x, Q^2]$ phase space as a function of F_5 itself, see Figure 5 (left). At lower x, F_5 values are high; notice that below $Q^2 = 1$, the non-perturbative regime takes place, while above $Q^2 = 1$ corresponds to the perturbative regime. Figure 5 (right) shows the ratio between having $F_5 = 0$ or $F_5 \neq 0$, the ratio is greater than 1; which is expected since F_5 is a subtracted component of the total cross section, see Equation 4; also, it means that there is a chance to disentangle an overall normalization change from a scaling of F_5.

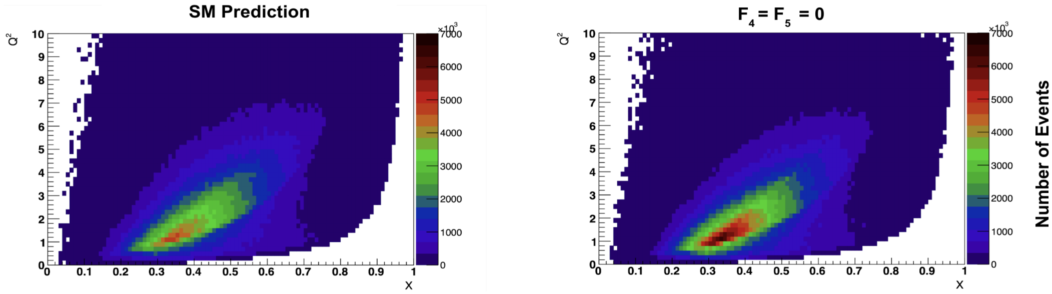

Figure 4. Left: $F_5(x, Q^2)$ phase space for the SM prediction. **Right**: $F_5(x, Q^2)$ phase space for the case when $F_4 = F_5 = 0$, which shows a greater region for nuclear interactions between $x = 0.2 - 0.5$.

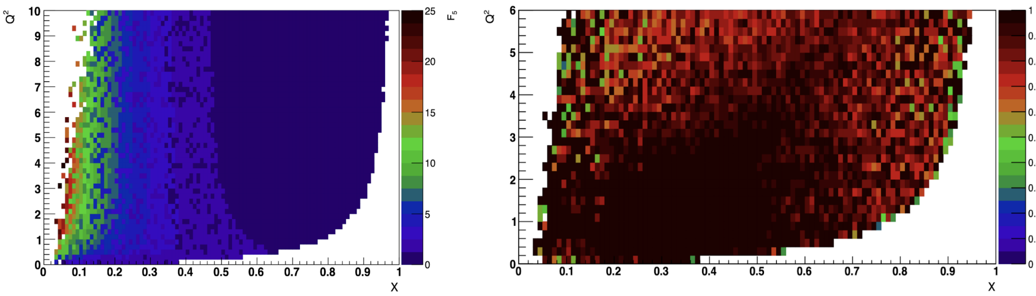

Figure 5. Left: $F_5(x, Q^2)$ phase space, F_5 is sensitive in values for x and Q^2 that wrap different interactions models. **Right**: the ratio between having $F_5 = 0$ or $F_5 \neq 0$, this ratio is greater than one, meaning that there is a chance to disentangle an overall normalization change from a scaling of F_5.

4. Discussion

There are new features that appear in the case of the ν_τA interactions as compared to ν_e and ν_μ interactions that contribute to modifying the cross sections, those are:

- Kinematic changes in Q^2 and E_l due to the presence of m_τ.
- The contributions due to the additional nucleon structure functions $F_4(x, Q^2)$ and $F_5(x, Q^2)$ in the presence of $m_\tau \neq 0$.
- As a function of Q^2, there is an enhancement that does not come just from a normalization, but due to the changes in the shape of the presence of m_τ.

Tau neutrinos play a central role in testing the lepton flavor universality violation of hints uncovered in flavor physics experiments, and DUNE will provide a unique opportunity to study the connections among neutrino flavors.

In order to obtain a reliable kinematic reconstruction, a machine learning approach is being reviewed, which is currently a technique called *panoptic segmentation* [8]. Panoptic segmentation combines *semantic segmentation*, which is the process of assigning a class label to each pixel, and *Instance segmentation*, which is the task of detecting objects in the image.

Funding: This research received no external funding.

Institutional Review Board Statement: Not applicable.

Informed Consent Statement: Not applicable.

Data Availability Statement: Not applicable.

Conflicts of Interest: The author declares no conflict of interest.

References

1. Abraham, R.M.; Alvarez-Muniz, J.; Argüelles, C.A.; Ariga, A.; Ariga, T.; Aurisano, A.; Autiero, D.; Bishai, M.; Bostan, N.; Bustamante, M.; et al. Tau neutrinos in the next decade: From GeV to EeV. *J. Phys. G Nucl. Part. Phys.* **2022**, *11*, 110501. [CrossRef]
2. Machado, P.; Schulz, H.; Turner, J. Tau neutrinos at DUNE: New strategies, new opportunities. *Phys. Rev. D* **2020**, *10*, 053010. [CrossRef]
3. De Gouvêa, A.; Kelly, K.J.; Stenico, G.V.; Pasquini, P. Physics with Beam Tau-Neutrino Appearance at DUNE. *Phys. Rev. D* **2019**, *1*, 016004. [CrossRef]
4. Albright, C.H.; Jarlskog, C. Neutrino production of M^+ and E^+heavy leptons. *Nucl. Phys. B* **1975**, *2*, 467–492. [CrossRef]
5. Jeong, Y.S.; Reno, M.H. Tau neutrino and antineutrino cross sections. *Phys. Rev. D* **2010**, *82*, 033010. [CrossRef]
6. Kretzer, S.; Reno, M.H. Tau neutrino deep inelastic charged current interactions. *Phys. Rev. D* **2002**, *66*, 113007. [CrossRef]
7. Andreopoulos, C.; Barry, C.; Dytman, S.; Gallagher, H.; Golan, T.; Hatcher, R.; Perdue, G.; Yarba, J. The GENIE Neutrino Monte Carlo Generator: Physics and User Manual. *arXiv* **2015**, arXiv:1510.05494.
8. Kirillov, A.; He, K.; Girshick, R.; Rother, C.; Dollár, P. Panoptic Segmentation. *arXiv* **2019**, arXiv:1801.00868.